Chapter 4

Circular polarisation and bandwidth

M. Haneishi and Y. Suzuki

Microstrip antennas are widely used as an efficient radiator in many communication systems [1]. One of the most interesting applications is their use for transmitting or receiving systems required for circular polarisation [2–5]. A circularly polarised microstrip antenna can be classified into two categories, e.g. single- or dual-fed types. The classification of an antenna is based upon the number of feeding points required for circularly polarised waves. The singly-fed antenna is useful, because it can excite circular polarisation without using an external polariser. Therefore, it is important to understand the radiation mechanism of the antenna. However, one of the most serious problem in such an antenna is the considerable narrowness of the bandwidth compared to ordinary microwave antennas. This is a serious problem for the practical application of this antenna. For this reason, it is also important to study some wideband techniques.

In this Chapter, the various types of circularly polarised antennas are first briefly introduced in Section 4.1. In Section 4.2, a simple design method for a singly-fed antenna is described together with some useful design data. This method is useful in understanding its radiation mechanism and to roughly design it. However, if the general radiation mechanism and an accurate design method are required, then the more exact treatment, developed in Section 4.3, is necessary. In Section 4.4, some considerations of mutual coupling are described. Finally, three kinds of wideband techniques are introduced in Section 4.5.

4.1 Various types of circularly polarised antennas

There are many types of circularly polarised (CP) printed antennas, which are widely used as efficient radiators in many communication systems. Fig. 4.1 shows basic arrangements for various types of CP-wave printed antennas. In this Section, we describe briefly techniques for designing such CP printed antennas.

4.1.1 Microstrip patch antennas

A microstrip antenna is one of the most effective radiators for exciting circular polarisation. A circularly polarised microstrip antenna is categorised into two types by its feeding systems: one is a dual-feed CP antenna with an external polariser such as 3 dB hybrid, and the other is a singly-fed one without a polariser. The classification of antennas is based upon the number of feeding point required for CP excitation.

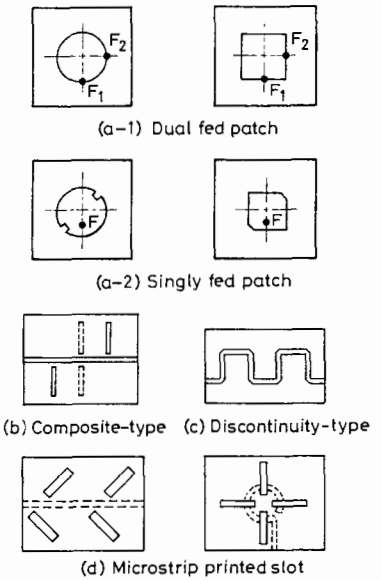

Fig. 4.1 *Various types of circularly polarised printed antennas*

(*a*) *Dual-fed CP patch antenna:* The fundamental configurations of a dual-fed CP patch antenna are shown in both Fig. 4.1 (a–1) and Fig. 4.2 (a). The patches are fed with equal amplitude and 90° out of phase by using an external polariser. As shown in the Figure, these antennas are also divided into two categories by the shape of an external polariser: one is the 3 dB hybrid type and the other is an offset-feeding one.

As is well known, a 3 dB hybrid such as a branch-line coupler produces fields of equal amplitude but 90° out of phase at its centre frequency. Therefore, setting the outputs of such a hybrid to the edges of the patch, the antenna acts as a CP radiator. It is necessary to note that each input terminal of a hybrid, however, gives an opposite sense of circular polarisation. In the present case, both the input VSWR and ellipticity bandwidth are broad, since a 3 dB hybrid, in general, has a broadband nature.

The other category is the offset-feeding CP antenna. Here, offset feeding lines, with one quarter wavelength longer than the other, are set at the edges of the patch, as shown in Fig. 4.2*a*. One of the most serious disadvantages of this type of antenna is the narrow bandwidth, since the frequency dependency of an offset-feeding line is greater than that of the usual hybrid.

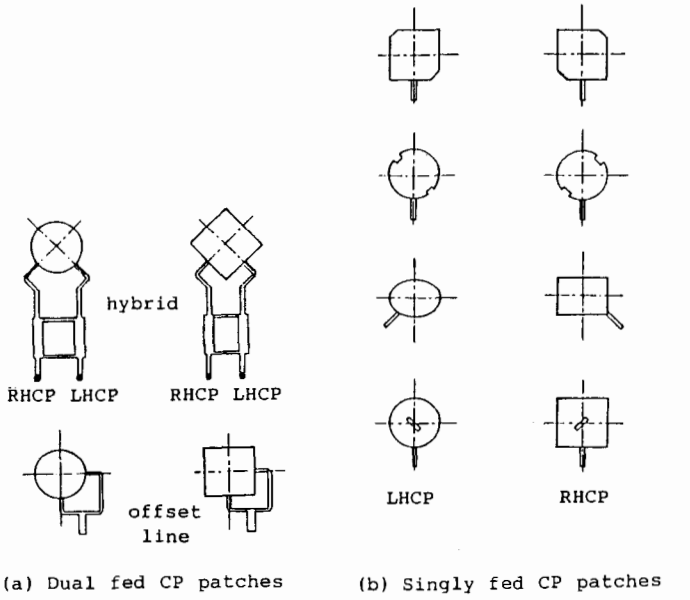

Fig. 4.2 *Typical arrangements for circularly polarised microstrip antennas*
LHCP: Left-hand circular polarisation
RHCP: Right-hand circular polarisation

(*b*) *Singly-fed CP patch antenna:* A singly-fed CP antenna may be regarded as one of the simplest radiators for exciting circular polarisation. The typical configurations of this antenna are shown in Fig. 4.2*b*. It is important to note that the generated mode in this case is usually excited in an electrically thin cavity region of the microstrip antenna. Accordingly, the operational principle of this antenna is based on the fact that the generated mode can be separated into two orthogonal modes by the effect of a perturbation segment such as a slot or other truncated segment [6–7,10–11]. Consequently, by setting the perturbation segment to the edge of the patch, the generated mode is separated into two

orthogonal modes 1 and 2. The typical amplitude and phase diagrams after perturbation are shown in Fig. 4.3, together with typical samples of antennas.

The radiated fields excited by these two modes are, in general, perpendicular to each other, and orthogonally polarised in the boresight direction. When the amount of perturbation segment is adjusted to the optimum value, modes 1 and 2 are excited in equal amplitude and 90° out of phase at the centre frequency, as shown in the Figure. This enables the antenna to act as a CP radiator in spite of single feeding. This antenna has several advantages compared to dual-fed ones and can excite CP radiation without using an external polariser. Design techniques will be described in detail in Sections 4.2 and 4.3.

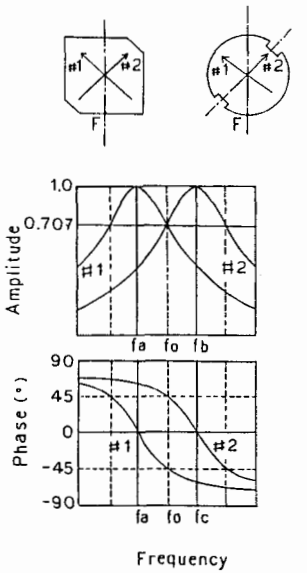

Fig. 4.3 *Amplitude and phase diagrams for singly-fed circularly polarised microstrip antennas*

4.1.2 Other types of circularly polarised printed antennas

In this section, we describe briefly the fundamental design procedures for others types of CP antennas.

(*a*) *Composite type of CP printed antenna:* Fig. 4.4*a* shows the fundamental configuration of a composite-type CP antenna [8]. The antenna is composed of the combination of a half-wavelength-long strip conductor and a slot in the ground plane. If the microstrip feeding line is short-circuited at $l = 0$, a standing-wave voltage V_l and current I_l occurs along the microstrip feeding line. In

the present case, on setting the radiating elements such as the strip and the slot to the maximum positions of V_l and I_l, these radiating elements radiate transverse and longitudinal electric fields E_{st} and E_{sl}, respectively, in the boresight direction. The fields E_{st} and E_{sl} can be excited in equal amplitude and at 90° out

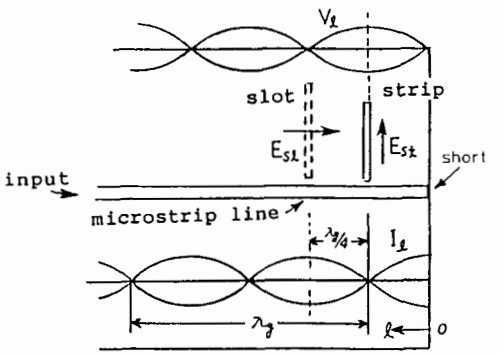

(a) Radiating element for composite-type circularly polarised printed antenna[8]

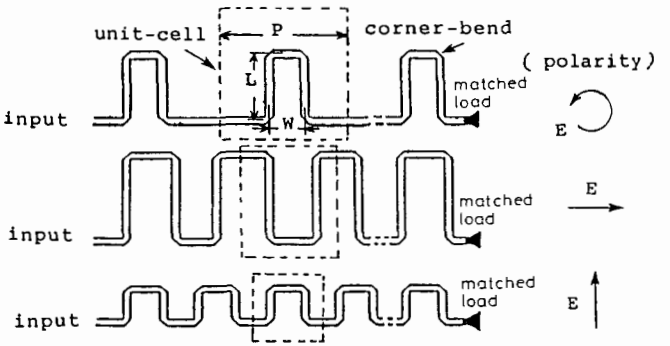

(b) Various arrangements of rampart line antennas[6]

Fig. 4.4 *Typical arrangements for travelling-wave-type printed antennas*

of phase, if the strip and the slot are spaced one-quarter wavelength apart and the coupling between the radiating element and feeder is controlled to be identical in value. Therefore, this type of antenna acts as CP radiator without using any external polariser. Details of design techniques for this antenna will be discussed in Chapter 13.

(*b*) *Discontinuity type of CP printed antenna:* A rampart-line antenna is a typical radiator for the discontinuity type [6,9]. Fig. 4.4*b* shows typical rampart line antennas that act as CP and LP radiators. Each radiator consists of a microstrip meander line having a series of corner bends. The antenna also has a matched load at the open end of the meander line. In this system, radiation occurs mainly from the discontinuity section of the meander line such as a corner bend. Therefore, both CP and LP rampart line antennas can be easily fabricated by controlling the length L, width W and period P of the meander line. If L, W and P are adjusted to $\lambda_g/2$, $\lambda_g/4$ and λ_g, respectively, for a unit cell of the meander line (λ_g is the wavelength of the travelling wave along the meander line), the antenna acts as a CP radiator. When $L = 2\lambda_g/3$, $W = \lambda_g/3$ and $P = 2\lambda_g/3$, the antenna radiates horizontal polarisation, while $L = W = \lambda_g/4$, $P = \lambda_g/2$ excites vertical polarisation, as shown in Fig. 4.4*b*. Details of the design procedure will be discussed in Chapter 13.

4.2 Simple design techniques for singly-fed circularly polarised microstrip antennas

This Section gives a brief description of design techniques for singly-fed radiators together with some useful experimental results. The approach is based on the variational method, and is useful for understanding the mechanism of CP radiation from such singly-fed radiators.

4.2.1 Rectangular type

In general, microstrip antennas are divided into two types by the shape of radiating element: rectangular type and circular type. However, since the rectangular patch antenna is considered to be a fundamental device for exciting CP radiation, the design techniques for this type are discussed first.

(*a*) *Fundamental configuration of rectangular CP-wave antenna:* The fundamental configurations of the antenna and its co-ordinate system are shown in Fig. 4.5. In type A, the feeding point F is placed on the x- or y-axis, whereas in type B, F is placed on the diagonal axis. In both cases, the perturbation segment Δs is set at an appropriate location in the patch element to excite CP radiation. Here, we describe briefly the sense of direction for the CP-wave. Right-hand or left-hand CP radiation can be achieved by setting feeding points at appropriate locations such as $F(\pm\varrho_0, 0)$ and $F(0, \pm\varrho_0)$, as shown in Fig. 4.6.

(*b*) *Effect of perturbation segment:* The effect of perturbation segment Δs for the type-A antenna is described first, since this type of radiator is a basic device for exciting CP radiation.

The eigen functions ϕ_a and ϕ_b, which are excited in an electrically thin cavity region of the square patch, are generally given mathematically by the following

equations, while a perfect magnetic wall is assumed as a boundary condition at the antenna peripheries ($x = \pm a/2, y = \pm b/2$);

$$\left.\begin{aligned} \phi_a &= V_0 \sin k\,x \\ \phi_b &= V_0 \sin k\,y \end{aligned}\right\} \tag{4.1}$$

where $V_0 = \sqrt{2}/a$ and $k = \pi/a$.

The eigen function ϕ_a is concerned with the field distribution of TM_{100} mode, and ϕ_b with that of TM_{010} mode. By setting the perturbation segment Δs at an appropriate position of the antenna, as shown in Fig. 4.5, two orthogonally polarised modes are excited in a cavity region of the antenna.

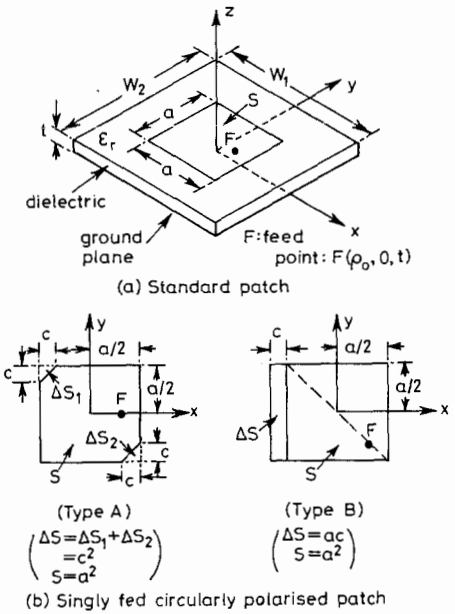

Fig. 4.5 *Fundamental configurations of singly-fed rectangular patches (From Reference 11)*

The new eigen function ϕ' and the new eigen value k', after perturbation by the segment, are determined by the following equations [11, 12, 15]:

$$\left.\begin{aligned} \phi' &= P\phi_a + Q\phi_b \\ k'^2 &= \frac{\iint_{s+\Delta s_1+\Delta s_2} (P\nabla\phi_a + Q\nabla\phi_b)^2\, dS}{\iint_{s+\Delta s_1+\Delta s_2} (P\phi_a + Q\phi_b)^2\, dS} \end{aligned}\right\} \tag{4.2}$$

where P and Q are unknown expansion coefficients of the new eigen function ϕ'.

The new eigen value k' of the antenna can be derived by employing the following matrix, since eqn. 4.2 is a variational-expression form:

$$\det \begin{vmatrix} k^2 + q_1 - k'^2(1 + p_1) & q_{12} - k'^2 p_{12} \\ q_{12} - k'^2 p_{12} & k^2 + q_2 - k'^2(1 + p_2) \end{vmatrix} = 0 \tag{4.3}$$

In case of the type-A antenna, the parameters in eqn 4.3, such as p_1, p_2, q_1, q_2, p_{12} and q_{12}, are expressed by the following equations [11]:

$$\left.\begin{aligned} q_1 &= q_2 = q_{12} = 0 \\ p_1 &= p_2 = 2(\Delta s/S) \\ p_{12} &= -2(\Delta s/S) \end{aligned}\right\} \tag{4.4}$$

Substituting eqn. 4.4 into eqn. 4.3, the new eigen values k_a' and k_b' for type A are given as

$$\left.\begin{aligned} k_a'^2 &= k^2(1 - 4\Delta s/S) \\ k_b'^2 &= k^2 \end{aligned}\right\} \tag{4.5}$$

where k_a' and k_b' correspond to the eigenvalues of the new orthogonal eigen functions, ϕ_a' and ϕ_b', respectively.

Using eqn. 4.5, new sets of resonant frequencies for the ϕ_a' and ϕ_b' modes are easily obtained as follows:

$$\left.\begin{aligned} f_a &= f_{0r} + \Delta f'_a = f_{0r}(1 - 2\Delta s/S) \\ f_b &= f_{0r} + \Delta f'_b = f_{0r} \end{aligned}\right\}$$

where f_{0r} is the resonant frequency for a normal square patch before perturbation, and $\Delta f_a'$ and $\Delta f_b'$ are the shifts of resonant frequencies for the ϕ_a' and ϕ_b' modes after perturbation.

Normalising the new eigen functions for the ϕ_a' and ϕ_b' modes, the unknown expansion coefficients P and Q are determined as follows [11, 12]:

For ϕ_a' mode,

$$\left.\begin{aligned} P_a &= (1/\sqrt{2})(1 - 2\Delta s/S) \simeq (1/\sqrt{2}) \\ Q_a &= (-1/\sqrt{2})(1 - 2\Delta s/S) \simeq (-1/\sqrt{2}) \end{aligned}\right\}$$

For ϕ_b' mode

$$P_b = Q_b = (1/\sqrt{2})$$

Finally, using eqns. 4.1, 4.2 and the expansion coefficient, the new eigen functions ϕ_a' and ϕ_b' are given in a closed form by

$$\left.\begin{aligned} \phi'_a &\simeq (\phi_a - \phi_b)/\sqrt{2} = V_0(\sin kx - \sin ky)/\sqrt{2} \\ \phi'_b &\simeq (\phi_a + \phi_b)/\sqrt{2} = V_0(\sin kx + ky)/\sqrt{2} \end{aligned}\right\} \tag{4.6}$$

The eigen values used in eqn. 4.6 are assumed to be $k_a' = k_b' = k$ by means of first-order approximation.

Furthermore, the turn ratios N_a' and N_b', which correspond to the energy distribution ratios for both the ϕ_a' and ϕ_b' modes after perturbation, are defined as [11]

$$\left.\begin{aligned} N'_a &= (\sqrt{S}/a)(\sin kx - \sin ky) \\ N'_b &= (\sqrt{S}/a)(\sin kx + \sin ky) \end{aligned}\right\} \tag{4.7}$$

In the case of the type-B antenna shown in Fig. 4.5, the eigen functions ϕ'_a, ϕ'_b and other parameters can also be derived by similar calculations employed for type A. The equations obtained by these calculations are as follows:

$$\left.\begin{aligned} p_1 &= p_2 = (3/2)(\Delta s/S) \\ p_{12} &= -(1/2)(\Delta s/S) \\ q_1 &= q_2 = (1/2)(\Delta s/S)k^2 \\ q_{12} &= +(1/2)(\Delta s/S)k^2 \\ k_a'^2 &= k^2(1 - 2\Delta s/S) \\ k_b'^2 &= k^2 \\ f_a &= f_{0r} + \Delta f'_a = f_{0r}(1 - \Delta s/S) \\ f_b &= f_{0r} + \Delta f'_b = f_{0r} \\ \phi'_a &= (\sqrt{2}/a)(1 - \Delta s/S)\sin kx \\ \phi'_b &= (\sqrt{2}/a)(1 - \Delta s/2S)\sin ky \\ N'_a &= \sqrt{S}\,\phi'_a \simeq \sqrt{2}\sin kx \\ N'_b &= \sqrt{S}\,\phi'_b \simeq \sqrt{2}\sin ky \end{aligned}\right\} \tag{4.8}$$

where $V_{00} = 1/a$ and $k = \pi/a$.

Using eqns. 4.1–4.7, we can derive the equivalent circuit for the type-A antenna. Furthermore, the equivalent circuit of the type-B antenna after perturbation can also be derived using the relations given in eqns. 4.8. The circuit for both the types of antennas is shown in Fig. 4.7. In this circuit, T'_A and T'_B represent ideal transformers having turn ratios N'_a and N'_b, and $\dot{V}_f$ is input voltage applied to the 1–1′ terminal.

(c) Condition required for CP-wave radiation: In this Section, conditions for exciting CP-wave radiation are determined by use of the preceding equivalent circuit. As is well known, the equivalent conductances G'_a and G'_b in the circuit are expressed as the sum of the radiation, dielectric and copper losses. However, in normal patches having adequate radiation efficiency above 90%, radiation loss is dominant compared with the other losses.

Consequently, the equivalent conductances G'_a and G'_b are mainly caused by the radiated fields resulting from the patch antenna. In other words, the induced voltages $\dot{V}_a$ and $\dot{V}_b$ generated on G'_a and G'_b can be assumed to correspond to the radiated fields caused by the orthogonal ϕ'_a and ϕ'_b modes.

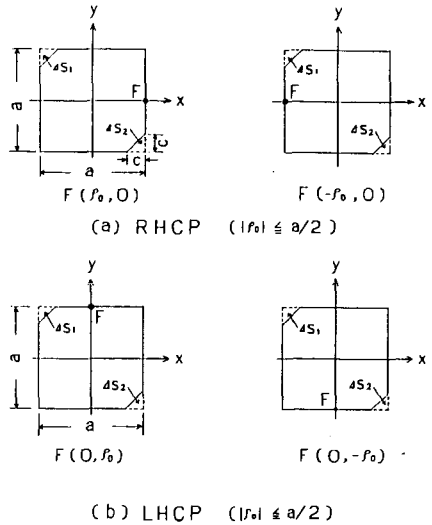

Fig. 4.6 *Feeding locations required for circular polarisation*
RHCP: Right-hand circular polarisation
LHCP: Left-hand circular polarisation
ϱ_0 = feed location

Applying network analysis to the equivalent circuit, the complex amplitude ratio $\dot{V}_a/\dot{V}_b$ in the two orthogonal modes is given as follows:

$$(\dot{V}_b/\dot{V}_a) = (N'_b/N'_a)*(\dot{Y}_a/\dot{Y}_b) = \left(\frac{N'_b}{N'_a}\right)\frac{\left\{\frac{f_a}{Q_0}+j\left(f-\frac{f_a^2}{f}\right)\right\}}{\left\{\frac{f_b}{Q_0}+j\left(f-\frac{f_b^2}{f}\right)\right\}} \tag{4.9}$$

where $\dot{Y}_a$ and $\dot{Y}_b$ are input admittances for the orthogonally polarised ϕ'_a and ϕ'_b modes, respectively. In addition, the unloaded Q factors in the above equation are expressed as $Q_{0a} = Q_{0b} = Q_0$ to first-order approximation, where Q_{0a} and Q_{0b} are the unloaded Q factors of the ϕ'_a and ϕ'_b modes.

From eqn. 4.9, radiation of CP waves by these radiators may be expected if

$(\dot{V}_b/\dot{V}_a) = \pm j$ is satisfied. Accordingly, these antennas act as a CP radiator by setting the relative amplitude and phase between the two orthogonal modes at $|\dot{V}_b/\dot{V}_a| = 1$ and $\arg(\dot{V}_b/\dot{V}_a) = \pm 90°$, respectively.

Applying the above conditions to eqn. 4.9, turns ratios are required to satisfy the relation $|N'_b/N'_a| = 1$. In addition, when this restriction is applied to the type-A antenna, it is necessary to place the feeding point F on the x-axis for $(N'_b/N'_a) = 1$. Contrariwise, the feeding point F is required to be placed on the y-axis by another restriction $(N'_b/N'_a) = -1$.

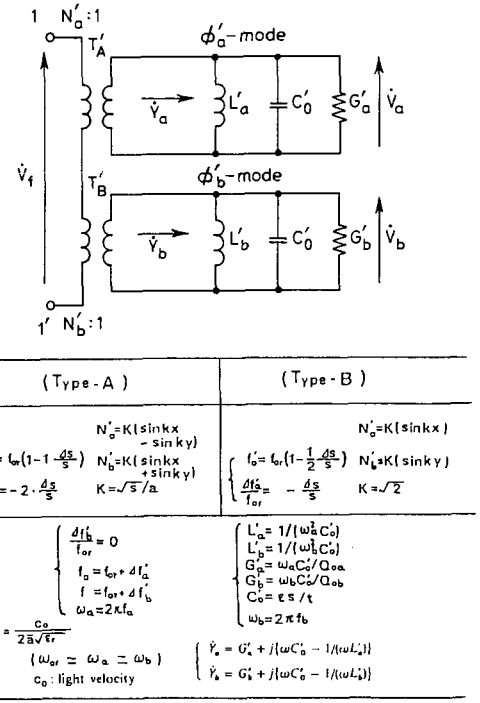

Fig. 4.7 *Equivalent circuit for rectangular circularly polarised patch antennas*

Setting the feeding point at each location, the expression for the complex amplitude ratio is shown as follows:

$$(\dot{V}_b/\dot{V}_a) = \pm\frac{\left(\frac{f_a}{Q_0}\right)+j\left(f-\frac{f_a^2}{f}\right)}{\left(\frac{f_b}{Q_0}\right)+j\left(f-\frac{f_b^2}{f}\right)}$$

By application of the CP conditions satisfying $|\dot{V}_b/\dot{V}_a| = 1$ and $\arg(\dot{V}_b/\dot{V}_a) = \pm 90°$ to the above equation, an important relation between Q_0 and $(\Delta s/S)$ is obtained as follows:

$$\frac{(Q_0^2 - 1)Q_0^2}{2Q_0^2 - 1}(M^2 + N^2) = MN\left\{1 + \frac{(2Q_0^2 - 1)MN}{M^2 + N^2}\right\} \tag{4.10}$$

where $M = (1 + m\Delta s/S)$, $N = (1 + n\Delta s/S)$, and m and n are the constants in $f_a = f_{0r}(1 + m\Delta s/S)$ and $f_b = f_{0r}(1 + n\Delta s/S)$.

In case of the type-A radiator, constants m and n are shown as $m = -2$ and $n = 0$, as mentioned previously. Substituting these values into eqn. 4.10, and carrying out some modifications of the equation, the most important expression for designing purposes is easily obtained as follows:

$$|\Delta s/S|Q_0 = 1/2 \tag{4.11}$$

This expression is simple in form but very useful for actual design of the type-A radiator.

Furthermore, in case of the type-B antenna, a basic equation for design can also be derived by the use of similar techniques, and the expression is as follows:

$$|\Delta s/S|Q_0 = 1$$

The relations for both basic expressions are illustrated in Fig. 4.8*b* by solid lines. They help to provide important design parameters such as the amount of perturbation $(\Delta s/S)$ required for CP radiation.

(d) Basic design procedures for CP-wave antennas: In designing CP-wave antennas, it is necessary to estimate the value of unloaded $Q(Q_0)$ as a function of substrate thickness t for an antenna. Therefore, theoretical values of Q_0 were calculated for a typical sample ($a = 9{\cdot}14$ mm, $t = 0{\cdot}6$ mm, $\varepsilon_r = 2{\cdot}55$) employing a commonly used technique [6, 10]. The theoretical values agreed well with the experimental ones, as shown in Fig. 4.8*a*. After determining the value of Q_0, the design of an antenna can be achieved by the following procedures:

(i) Using the relations shown in Fig. 4.8*a*, the unloaded $Q(Q_0)$ of the square patch is chosen so as to ensure that the radiation efficiency η of the patch will exceed 90%.
(ii) The amount of perturbation $(\Delta s/S)$ required for CP-wave excitation is determined using the relation between Q_0 and $(\Delta s/S)$ shown in Fig. 4.8*b*.
(iii) Finally, the input impedance of the test antenna is matched to that of the feed network by the offset loading technique of coaxial probe or using a quarter-wavelength transformer.

The approaches described above are performed without considering the effect due to fringing fields. However, when the fringing effect is taken into consideration [6], the procedures help to provide more accurate design parameters required for CP radiation.

(e) Radiation characteristics of CP antennas: In order to verify the validity of the above design procedures, typical samples of CP antennas were fabricated and tested at X-band. These antennas were fed with a coaxial probe to avoid the influence of unwanted radiation from the feeding networks. The radiation

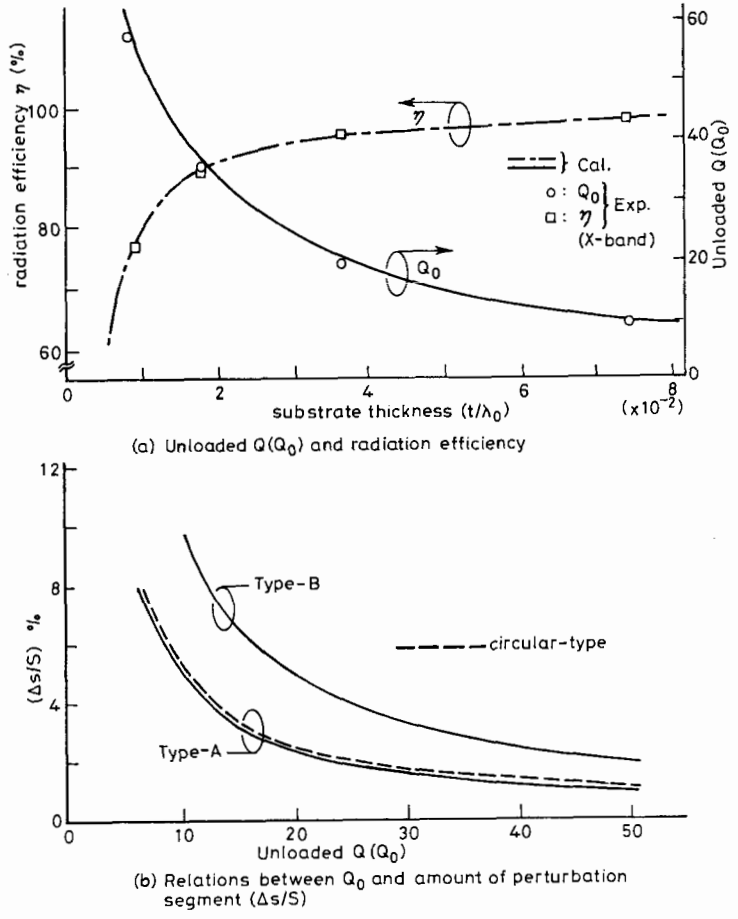

Fig. 4.8 *Fundamental design chart for singly-fed circularly polarised patch antennas*

patterns measured by a spinning dipole are shown in Fig. 4.9. As seen from the Figure, the ellipticity of the test antenna is less than 0·5 dB in the boresight direction. Furthermore, the ellipticity is within 1·5 dB in the desired angular region of 45°.

Fig. 4.10 shows the measured impedance characteristics of the typical CP-wave antenna. From these results, it is found that loop 1 in the impedance-plot locus depends on the degree of mode separation; namely, loop 1 becomes larger in area with an increase in mode separation, and converged to a point when the mode separation is reduced. In any case, however, the best ellipticity can be obtained at or near the peak of loop 1 in the impedance locus.

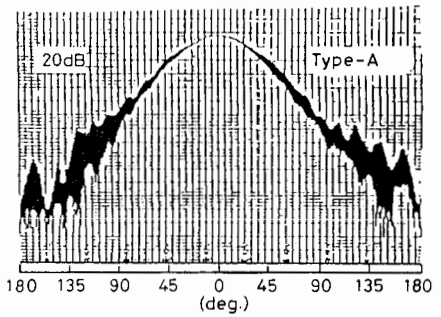

(a) Pattern of type-A circularly polarised patch

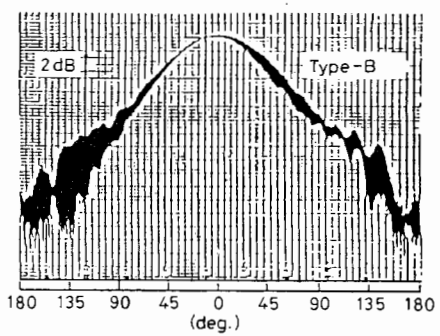

(b) Pattern of type-B circularly polarised patch

Fig. 4.9 *Typical radiation patterns of rectangular singly-fed circularly polarised patches, (From Reference 11)*
$[t/\lambda_0 = 0{\cdot}018,\ \varepsilon_r = 2{\cdot}55,\ \tan\delta = 0{\cdot}0018,\ (\varrho_0/(a/2)) = 0{\cdot}3,\ W_1 = W_2 = \lambda_0$ (Fig. 4.5*a*), and X-band

4.2.2 Circular type

This Section gives a brief description of a design technique for a circular antenna. The geometry and feed system of the antenna are shown in Fig. 4.11. In this antenna, the perturbation segment Δs is also located at a specific location. The degenerate mode is also separated from the dominant mode (TM_{110}) in the antenna into two orthogonal modes by the effect of the perturbation segment.

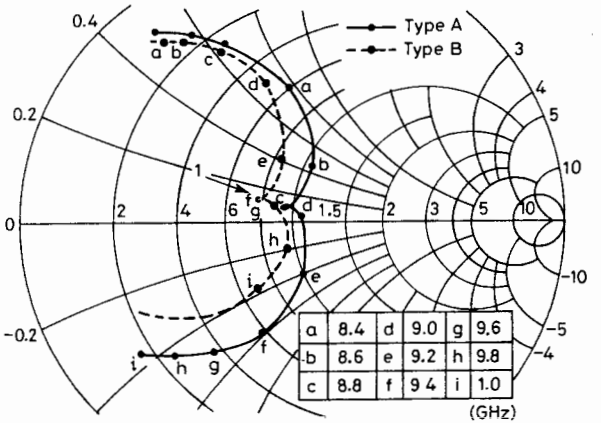

Fig. 4.10 *Typical measured impedance characteristics for rectangular singly-fed circularly polarised patch antennas (From Reference 11)*
$t/\lambda_0 = 0{\cdot}018,\ \varepsilon_r = 2{\cdot}55,\ \tan\delta = 0{\cdot}0018$ and $(\varrho_0/(a/2)) = 0{\cdot}3$

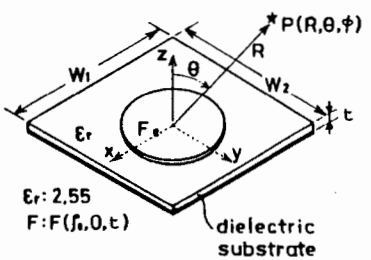

(a) Standard patch

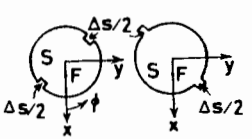

(b) circular CP elements

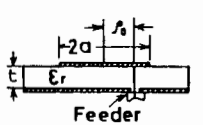

(c) Feeding system

Fig. 4.11 *Fundamental configurations for circular singly-fed circularly polarised patch antennas*

The equivalent circuit after perturbation is useful for network analysis of the radiator. Fortunately, the equivalent circuit for the antenna can easily be obtained by employing the same procedures as in the previous Section. The equivalent circuit for the antenna after perturbation is shown in Fig. 4.12 [7].

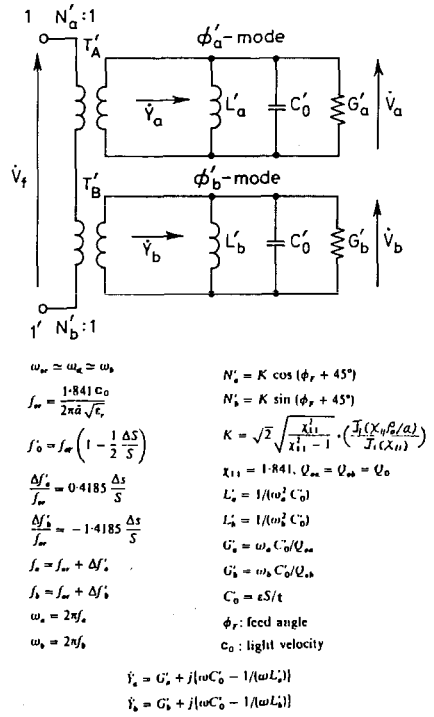

Fig. 4.12 *Equivalent circuit for circular singly-fed circularly polarised patch antenna (From Reference 7)*

The CP-radiation condition for the circular patch can be determined using the above equivalent circuit. Namely, by application of the design procedures employed for the rectangular patches, the CP-wave condition for the circular one is obtained as

$$Q_0|\Delta s/S| = 1/\chi_{11}$$

where $(\Delta s/S)$, Q_0 and χ_{11} correspond to the amount of perturbation, the unloaded Q and the eigen value of the dominant TM_{110} mode, respectively.

Using the above equation, the relation that gives a CP-radiation condition for the antenna is indicated by the dotted-line in Fig. 4.8*b*. This Figure helps to

provide important design parameters such as the amount of perturbation required for CP-wave radiation. In actual design, however, it is important to note that the Q_0 of the circular patch becomes equivalent to that of the rectangular one, if both the patches are designed to have the same resonant frequencies.

For this reason, the circular CP antennas can be designed as easily as rectangular antennas by employing the relations shown in Fig. 4.8. However, the fringing effect is disregarded in above approaches. If the effect of fringing fields is taken into consideration [6], the experimental results agree well with theory, as mentioned below.

In order to verify the validity of the design procedure, some circular CP patches were fabricated and tested at X-band. These samples were fabricated using a substrate consisting of copper-clad 0·6 mm-thick Teflon glass fibre with a dielectric constant of 2·55 and a loss tangent of approximately 0·0018. The boresight ellipticity of the test antenna was about 0·5 dB or less, and the radiation patterns revealed as a high a level of performance as those of the rectangular patch. In addition, the ellipticity bandwidth within 3 dB was about 1% with a substrate thickness of $(t/\lambda_0) = 0{\cdot}019$, and about 2% with a thickness of $(t/\lambda_0) = 0{\cdot}037$. These results indicate that, as the substrate thickness increases, the ellipticity bandwidth also increases.

Furthermore, the trend of the impedance locus plot of the antenna coincided with that of the rectangular one shown in Fig. 4.10.

4.3 More exact treatment of singly-fed circularly polarised microstrip antennas

The patch radiator can easily be modified from a circular, square or rectangular shape so as to excite circularly polarised waves with a single feed as mentioned previously. In addition to these shapes [4, 5], a specially shaped pentagonal [2], triangular [13] or elliptical radiator [3] can also radiate circular polarisation. Furthermore, it has been known that the polarisation and resonant frequency can be conveniently controlled by inserting posts at suitable locations within the patch boundary [14]. However, it is not generally easy to analyse such antennas accurately, so designers are often forced to use cut-and-try methods to realise the desired characteristics.

In this Section, an analysis, based on variational method [15] and modal expansion technique [16], is briefly summarised for an arbitrarily shaped microstrip antenna with multi-terminals before starting the discussion concerning a singly-fed circularly polarised antenna. Using the results of analysis the conditions for producing circularly polarised waves are derived, and then it is shown that a microstrip antenna, in general, can radiate circularly polarised waves at two kinds of frequencies with a single feed. Finally, one design example is given in order to confirm experimentally the several theoretical predictions concerning the feed points and the operating frequencies to radiate them.